Interaction of class A amphipathic helical peptides with phospholipid unilamellar vesicles

Jeffrey A. Gazzara,* Michael C. Phillips,† Sissel Lund-Katz,† Mayakonda N. Palgunachari,§ Jere P. Segrest,§ G. M. Anantharamaiah,§ and Julian W. Snow[1,*]

Department of Chemistry,* Philadelphia College of Pharmacy and Science, Philadelphia PA 19104; Department of Biochemistry,† Allegheny University of the Health Sciences, Philadelphia, PA 19129; and Departments of Medicine and Biochemistry and Molecular Genetics and the Atherosclerosis Research Unit,§ University of Alabama at Birmingham Medical Center, Birmingham, AL 35294

Abstract The exchangeable apolipoproteins are important in determining the structure/function properties of lipoproteins. These proteins typically contain varying amounts of amphipathic helices. Five model peptides, 18A, Ac-18A-NH_2, Ac-18R-NH_2, 37pA, and 37aA, have been designed to investigate variations of the amphipathic α-helix structural motif on their lipid-binding properties. These include the 18-residue peptides, 18A and Ac-18A-NH_2, examples of class A helices, and Ac-18R-NH_2, which has the positions of acidic and basic residues interchanged relative to 18A. Three larger peptides were also studied: 36A, a dimer of 18A, 37pA and 37aA, dimers of 18A coupled by Pro (18A-Pro-18A) and Ala (18A-Ala-18A), respectively. We report here the results of a thermodynamic characterization of the binding properties of these peptides to small unilamellar vesicles of POPC. Partition coefficients, K_p, were determined by fluorescence spectroscopy and binding enthalpies, ΔH, by titration calorimetry. These parameters were used to obtain the free energies, ΔG^0, and entropies, ΔS^0, of binding. The results of this study indicate K_p values on the order of 10^5, with interactions being enthalpically but not entropically favored in all cases. The presence of positively charged residues at the interface (18A and Ac-18A-NH_2) enhances binding but has little effect on the extent of bilayer penetration. The presence of tandem repeats decreases lipid affinities for these small, highly curved bilayers. Our results are consistent with the idea that interaction appears to be confined largely to the surface, with some degree of penetration of the hydrophobic face of the helix into the interior of the bilayer.—**Gazzara, J. A., M. C. Phillips, S. Lund-Katz, M. N. Palgunachari, J. P. Segrest, G. M. Anantharamaiah, and J. W. Snow.** Interaction of class A amphipathic helical peptides with phospholipid unilamellar vesicles. *J. Lipid Res.* 1997. **38:** 2134–2146.

Supplementary key words amphipathic helix • phospholipid vesicles • fluorescence • titration calorimetry • circular dichroism

The structure and metabolism of plasma lipoproteins are modulated by the apolipoproteins associated with their surface. For example, apolipoprotein A-I (apoA-I), the major protein of high density lipoproteins (HDL), consisting of a single polypeptide chain of 243 amino acids (1), is critical for the function of HDL in reverse cholesterol transport. An interesting aspect of the exchangeable plasma apolipoproteins, such as apoA-I, is that their lipid-binding properties appear to be modulated to a great extent by the amphipathic α-helix structural motif (2–4). The lipid affinity of these helices is influenced by such physicochemical properties as the hydrophobicity of the amino acid side chains on the nonpolar face, the distribution of charged residues around the helix axis, the magnitude of the helix hydrophobic moment, and the length of the helix (3, 4). ApoA-I contains eight 22-mer amphipathic helical domains, the majority of which are characterized as class A, having positively charged residues at the polar-nonpolar interface and negatively charged residues at the center of the polar face (3). The quantitative basis for the lipid affinities of proteins or peptides containing amphipathic α-helical domains is not well understood at present.

To develop a detailed molecular understanding of the lipid affinity of amphipathic helices and the exchangeable apolipoproteins, several synthetic model peptides have been designed. The 18-residue model peptide, 18A, has the amino acid sequence Asp Trp Leu Lys Ala Phe Tyr Asp Lys Val Ala Glu Lys Leu Lys Glu Ala Phe, characterizing it as class A (5, 6). 18A has the ability to activate the plasma enzyme lecithin:cholesterol acyltransferase (LCAT), solubilize DMPC bilayers

Abbreviations: apo, apolipoprotein; CD, circular dichroism; DMPC, 1,2-dimyristol-*sn*-glycero-3-phosphocholine; EDTA, ethylenediamine-tetraacetate; e.u., entropy units; Gdn.HCl, guanidine hydrochloride; HDL, high density lipoprotein; K_p, partition coefficient; LCAT, lecithin:cholesterol acyltransferase; MLV, multilamellar vesicle(s); NATA, N-acetyltryptophanamide; POPC, 1-palmitoyl-2-oleoyl-*sn*-glycero-3-phosphocholine; PBS, phosphate-buffered saline; SUV, small unilamellar vesicle(s).

[1]To whom correspondence should be addressed.

to form discs (4), and compete with apoA-I for the surface of HDL (6, 7). The helical wheel representation of 18A shows four positively charged Lys residues at the nonpolar-polar interface of the amphipathic helix and a total of four negatively charged Asp and Glu residues at the center of the polar face (8). Results of ^{13}C NMR studies with peptide-phospholipid complexes are consistent with the idea that charged residues are distributed about the polar face of the helix in this manner (9). The location of these charged residues has been stated to be significant for determining the free energy of association and depth of bilayer penetration of the helix (''snorkel hypothesis'', 3, 4). The formal charges at the amino and carboxyl termini of 18A interact adversely with the helical dipole, resulting in a decrease in helicity that affects the ability of the peptide to mimic more closely the properties of apoA-I (6, 10). Derivatization of the amino (acetyl) and carboxyl (amide) termini removes these charges, thereby stabilizing the helix in Ac-18A-NH_2 by about 1.3 kcal per mole of residue compared to 18A, which results in large increases in helicity both in solution and when bound to lipid (6).

To investigate the importance of charge distribution in 18A (and Ac-18A-NH_2) and understand the role of interfacial Lys residues in lipid association, a modified version of Ac-18A-NH_2, with the positions of the charged residues reversed, was synthesized (Ac-18R-NH_2); the sequence is Ac-Lys Trp Leu Asp Ala Phe Tyr Lys Asp Val Ala Lys Glu Leu Glu Lys Ala Phe-NH_2. The helical wheel diagram representation of this peptide shows four negatively charged amino acid residues at the polar-nonpolar interface, and positively charged residues at the center of the polar face. Also as apoA-I has tandem amphipathic helical repeats coupled by Pro residues, the model peptides 37pA and 37aA were designed. 37pA, a dimer of 18A linked by Pro (18A-Pro-18A), mimics many properties of apoA-I (8, 7, 11). It has been shown that the linking of two amphipathic helices by Pro increases the lipid-binding ability relative to the individual helices (8, 12). The model peptide 37aA is also a dimer of 18A, but linked by an Ala (18A-Ala-18A). The Pro or Ala residues (37pA or 37aA) cause the polar-nonpolar interfaces of the fully helical, 18-residue, segments to be twisted 100° out of register, or almost perpendicular to each other (13). The structures of the particles formed by interaction of these molecules with phospholipid have been studied extensively by some of us (for reviews, see 3–5).

This study was performed with the synthetic phospholipid, 1-palmitoyl-2-oleoyl-*sn*-glycero-3-phosphocholine (POPC). This lipid was chosen because its gel-to-liquid crystalline transition temperature is below 0°C, and also because its fatty acyl chains are similar to those of phospholipids of lipoproteins (14). The POPC was used to prepare small unilamellar vesicles (SUV) that were homogeneous in diameter (20 nm) as well as composition. Fluorescence spectroscopy was used to monitor the binding process. As the binding of peptides to fluid phospholipids occurs with an appreciable change in enthalpy, ultrasensitive titration calorimetry was utilized to determine the enthalpy of interaction for these model peptides at 25°C. We report here the results of a quantitative thermodynamic characterization of the effects of varying the location of charged residues about the polar face, and of modifying helix length on the lipid affinity and depth of bilayer penetration for model amphipathic α-helices.

MATERIALS AND METHODS

Materials

Peptides 18A, Ac-18A-NH_2, Ac-18R-NH_2, 36A, 37pA, and 37aA were synthesized by solid-phase methods and purified as described previously (6–8). 1-Palmitoyl-2-oleoyl-*sn*-glycero-3-phosphocholine was purchased from Avanti Polar Lipids, Inc. (Alabaster, AL) and used without further purification. Sodium chloride, disodium ethylenediamine-tetraacetate (EDTA), sodium dihydrogen phosphate monohydrate, anhydrous sodium hydrogen phosphate, potassium iodide, and sodium thiosulfate were purchased from Fisher Scientific Company (Fair Lawn, NJ). Acrylamide (purity > 99.9%) and guanidine hydrochloride (Gdn.HCl, purity ≥ 99%) were obtained from Bio-Rad (Richmond, CA) and GIBCO BRL (Gaithersburg, MD), respectively. Indole, N-acetyltryptophanamide, and (1S)-(+)-10-camphorsulfonic acid were purchased from Sigma Chemical Co. (St. Louis, MO).

Preparation of peptide solutions

The peptide solutions were prepared by dissolving the peptide in 6 M Gdn.HCl and dialyzing extensively against phosphate-buffered saline (PBS, pH 7.4; $NaH_2PO_4 \cdot H_2O$ 5.81 mM, Na_2HPO_4 9.19 mM, NaCl 145 mM) using 1000 MW cutoff dialysis bags. All the experiments described below were conducted with the same buffer system. Peptide concentrations were determined in buffer by measuring the absorbance at 280 nm (ϵ_{280}(18A, Ac-18A-NH_2, Ac-18R-NH_2) = 6800 M^{-1} cm^{-1}; ϵ_{280}(36A) = 13600 M^{-1} cm^{-1}, ϵ_{280} (37aA, 37pA) = 13500 M^{-1} cm^{-1}).

Preparation and characterization of phospholipid vesicles

SUV were prepared as follows: 16 mL of a solution of POPC in chloroform (20 mg/mL) was placed in a 15-mL Corex test tube in four 4-mL aliquots. After each

addition, the chloroform was removed under a stream of N_2 leaving a thin film of lipid on the walls of the tube. Any remaining solvent was removed by drying under vacuum at 40°C for 2 h. The dried lipid was hydrated with 5 mL of a solution containing 150 mM NaCl, 1 mM EDTA, then the suspension was vortexed to give a final lipid concentration of about 64 mg/mL. The lipid was dispersed by sonication with a Branson sonifier (model 250, equipped with a tapered microtip) under N_2 in an ice bath keeping the lipid above the POPC gel-liquid crystalline transition (−5°C). The dispersion was sonicated with an output of 80 watts in 5-min intervals, separated by 2-min cooling periods, for 50 min. The method of Barenholz et al. (15) for the isolation of the SUV from the dispersion was used. The multilamellar vesicles (MLV), undispersed lipid and titanium were removed by centrifuging at 40,000 rpm (106,000 *g* at r_{av}) for 2 h at 5°C, using a Beckman L5-50B ultracentrifuge equipped with a Ti50 rotor. The upper one-third of the supernatant containing the SUV was carefully removed with a syringe and used for the experiments described below. A portion of the supernatant was subjected to gel filtration on a calibrated Superose 6 Pharmacia column. Approximately 95% of the lipid was found in a single peak corresponding to SUV with a Stokes' radius of approximately 10.0 nm.

The molecular weight of the SUV was calculated using the following formula (16)

$$MW = \frac{4\pi r_e^3 N}{3V_V} - \frac{4\pi(r_e - d)^3 N}{3\rho} \qquad Eq.\ 1)$$

where r_e is the external radius in cm, d is the bilayer thickness (2.94×10^{-7} cm), N is Avogadro's number, V_v is the partial specific volume of egg phosphatidylcholine (0.9986 cm^3/g), and ρ is the specific volume of water (1 cm^3/g). The phospholipid concentration was determined spectrophotometrically by measuring the absorbance at 254 nm ($\epsilon_{254} = 88.9\ M^{-1}\ cm^{-1}$) with a Perkin-Elmer Lambda-6 spectrophotometer. This spectrophotometric assay was compared to a phosphorus assay (17) and was found to agree with it. The concentration of SUV was calculated by dividing the concentration of lipid by the number of moles of POPC per vesicle (mols of POPC/mol of SUV = 2.1×10^3).

Fluorescence spectroscopy

Fluorescence studies were performed with a Perkin-Elmer LS-5B luminescence spectrometer equipped with a thermostatically controlled cell holder at 25°C. Spectra were obtained with an excitation wavelength of 280 nm and recorded from 290–450 nm at 1-nm intervals. The partition coefficients, K_P, for the model peptides were determined from results of experiments in which peptide solutions at concentrations between 2–3 μM were titrated with small aliquots of SUV at concentrations of about 1.5 μM. All spectra were corrected for light scattering from the added lipid dispersion by digital subtraction of the appropriate SUV blanks. The Trp fluorescence intensities, F_I, for each addition were taken as areas under the emission spectra. These values were then corrected for dilution and normalized with respect to the fluorescence intensity of the peptide in buffer, F_B. The data were fit to the partitioning model described in the Appendix. Fluorescence quenching experiments were performed with potassium iodide (KI) and acrylamide solutions (4 M each). The KI contained 1 mM sodium thiosulfate ($Na_2S_2O_3$) to prevent I_3^- formation (18). To minimize absorptive screening by the acrylamide, an excitation wavelength of 295 nm was used for these experiments. Aliquots of quencher (15 μL) were added to 3 mL of 6 μM peptide solution and vortexed. After each addition of quencher the fluorescence intensity was measured at the emission maximum and corrected for dilution. For acrylamide quenching, intensity values were also corrected for the absorptive screening effect with the following equation (19)

$$f_{exc} = 2.3\frac{A}{1 - 10^{-A}} \qquad Eq.\ 2)$$

where f_{exc} is the absorptive screening correction factor and A is the absorbance of quencher at the exciting wavelength ($\epsilon_{295} = 0.25\ M^{-1}\ cm^{-1}$). The fluorescence quenching data were plotted as $(F_0/F) - 1$ versus [Q] where F_0 and F are the fluorescence intensities in the absence and presence of quencher, respectively, and [Q] is the quencher concentration. These plots were analyzed according to the Stern-Volmer equation for collisional quenching (20)

$$\frac{F_0}{F} = K_{SV}[Q] + 1 \qquad Eq.\ 3)$$

where K_{SV} is the Stern-Volmer constant for the collisional-quenching process. For plots that did not display considerable static quenching, the initial slopes were used to determine K_{SV}. When considerable static quenching was observed, these data were analyzed according to the modified Stern-Volmer equation (20) where V is the static quenching constant.

$$\frac{F_0}{F} = (K_{SV}[Q] + 1)e^{V[Q]} \qquad Eq.\ 4)$$

Circular dichroism

The far-UV CD spectra were recorded with a computer-interfaced JASCO J-41 A spectropolarimeter, which was calibrated with (1S)-(+)-10-camphorsulfonic acid (21). The spectra were measured from 260–

190 nm at 1-nm intervals and 1-nm bandwidth at 25°C. All CD spectra were baseline-corrected and signal-averaged by adding four scans each with 1 sec averaging per point and a scan speed of 100 nm/min. A 0.1-cm pathlength cell was used to obtain the spectra with peptide concentrations at 50 μM. The mean-residue ellipticity, $[\theta]$ (deg cm^2 dmole^{-1}), was calculated using

$$[\theta] = \frac{\theta(\mathrm{MRW})}{10\mathrm{Cl}} \qquad Eq.\ 5)$$

where, θ is the observed ellipticity in degrees, MRW is the mean residue weight of the peptide, C is the concentration of peptide in g/mL, and l is the cell path length in cm. The following equation was used to estimate the percent helicity of the peptide (22).

$$\%\alpha - \text{helicity} = \frac{(-[\theta]_{222} + 3000)}{(36000 + 3000)} \times 100 \qquad Eq.\ 6)$$

where, $[\theta]_{222}$ is the mean residue ellipticity at 222 nm.

Titration calorimetry

Enthalpies of peptide binding to SUV were measured with a MicroCal OMEGA titration calorimeter (MicroCal, Northampton, MA) using acquisition software supplied by MicroCal. Samples were dialyzed simultaneously and extensively against the same PBS buffer, using 1000 MW cutoff dialysis bags, to ensure buffer match, then were degassed under vacuum prior to use. Measurements were made at 25°C by titrating 10.0-μL aliquots of peptide solution, at concentrations between 350–400 μM, into the cell (1.3655 mL) containing an excess of lipid, at concentrations >16 mM, to ensure quantitative binding of peptide to vesicle. The concentration at which lipid is in excess was determined by injecting peptide into several SUV concentrations. When SUV are in excess, all injections yield similar ΔH values. Mixing of reactants was accomplished by rotating the syringe, whose end was fashioned into a paddle, at 400 RPM. The average enthalpies of binding for each peptide were obtained from six injections. These enthalpies were corrected for enthalpies of peptide dilution and dissociation at 25°C; these values were determined by titrating peptide into buffer alone.

Treatment of data

Experimental parameters determined by either nonlinear curve fitting or initial slope method were obtained using the Marquardt-Levenberg algorithm, with the SigmaPlot software package by Jandel Scientific (San Rafael, CA). The corresponding standard deviations, σ were calculated from the standard error of the fit and the number of data points, n, from σ = standard error ✓n. Precision of parameters was confirmed by repeating experiments no less than three times. Standard deviations of parameters calculated from experimental parameters were determined by calculating the propagated errors.

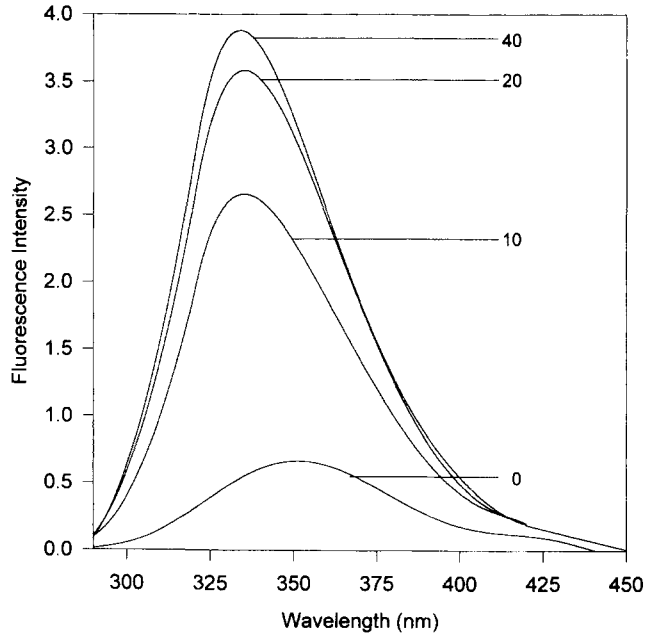

Fig. 1. Effect of SUV on the intrinsic fluorescence of 18A for POPC/peptide molar ratios of 0–40 at 25°C. The spectra are corrected for light scattering but not for dilution.

RESULTS

The 18-residue peptides 18A, Ac-18A-NH_2, and Ac-18R-NH_2, each contain a single Trp at the no. 2 position; the 37-residue peptides, 37pA and 37aA contain 2 Trp residues at positions no. 2 and 21 (36A at no. 2 and 20). These Trp residues were incorporated in the peptides as probes of peptide-phospholipid interaction because of the known sensitivity of their fluorescence properties (λ_{max} and intensity) to the polarity of their microenvironment (23). **Figure 1** demonstrates a dramatic increase in fluorescence intensity and a blue shift from 348 to 334 nm for 18A with the addition of POPC SUV to the peptide solution, indicating an interaction of monomeric peptide with the hydrophobic interior of the vesicle bilayer (24). We determined that peptides were monomeric at the low concentrations used in the fluorescence studies, prior to addition of vesicles, in a separate study in which we subjected peptide solutions at 25 μM first to cross-linking with dimethyl suberimidate, then to electrophoresis on calibrated, high-density polyacrylamide gels (M. Parmer and S.

Lund-Katz, unpublished results). Additionally, the concentration-dependence of the ellipticity at 222 nm indicated that peptides only self-associate at concentrations above 25 (6). 18A is capable of forming discs when complexed with DMPC, as was mentioned above; however, with POPC we observed no differences in migration patterns between vesicles and peptide-vesicle complexes on calibrated, Superose 6 columns, indicating that disc formation was not occurring under conditions used in these studies (peptide concentrations less than 5 μM, data not shown). Variations of these control experiments were performed in which the migration of POPC SUV, using tritiated phospholipid, was followed on Sepharose CL-6B columns by monitoring radioactivity. No difference in migration was observed for SUV in the absence or presence of representative 18-residue (Ac-18A-NH_2) or 37-residue (37pA) peptides (data not shown). Additionally, electron microscopic examination of SUV-peptide complexes with negative staining, using sodium phosphotungstate, showed no evidence of characteristically stacked or individual discs (data not shown).

Increases in fluorescence intensity and blue shifts were observed for all the peptides except 36A, which showed a decrease in intensity in the presence of vesicles, as was observed by others (13). A single measure of peptide-vesicle interaction was taken by determining the area under an emission spectrum (F_L). This area was then normalized to the area obtained for the same peptide solution prior to the addition of vesicles, yielding a unitless parameter, F_L/F_B (see Materials and Methods). This measure of binding indicates that it is saturable for all the peptides, except 36A (**Fig. 2**), which was not included in this study due to its failure to produce an increase in fluorescence intensity in the presence of vesicles. This was likely due to enhanced self-association because the nonpolar faces of 36A molecules aligned next to each other with their helical axes parallel, are capable of interacting with each other along the entire length of the molecules (13).

Previous studies have reported the lipid affinities of apolipoproteins in terms of equilibrium binding constants (24–26). However, due to the absence of distinct binding sites on the vesicle surface, it seems more appropriate to treat the peptide-SUV interaction as an equilibrium partitioning between the aqueous and lipid phases (27, 28). Accordingly, we have developed a partition model that expresses the peptide-vesicle interaction in terms of a (unitless) partition coefficient, $K_P = X_P^L/X_P^A$, the ratio of peptide mole fractions in the lipid and aqueous phases (see Appendix). This model has also been used to obtain stoichiometric parameters that characterize the peptide-SUV interactions (**Table 1**).

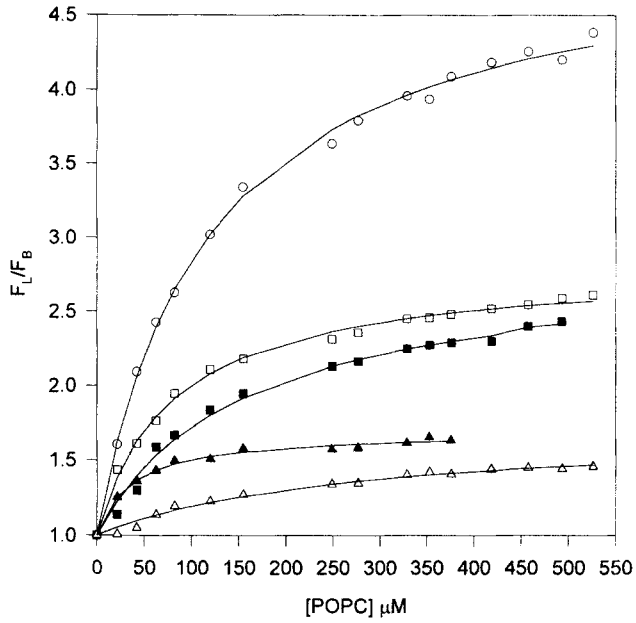

Fig. 2. Equilibrium binding isotherms for model peptides titrated with SUV at 25°C. The normalized fluorescence intensities, F_L/F_B, for 18A (■), Ac-18A-NH_2 (▲), Ac-18R-NH_2 (△), 37pA (□), and 37aA (○) were plotted as a function of lipid concentration. Partition coefficients, K_p, for each peptide were determined by curve fitting the respective binding isotherms (see Methods and Appendix).

The K_P values were converted to standard free energies of partitioning, ΔG^0, according to $\Delta G^0 = -RTlnK_P$. The K_P values obtained by fitting the data of Fig. 2 to this model (Table 1) are large, on the order of 10^5, with corresponding standard free energies of partitioning ranging from −7.3 to −8.4 kcal/mol (**Table 2**).

The increases in F_L/F_B for the unblocked peptides (18A, 37pA, and 37aA) are much larger than for both

TABLE 1. Partition coefficients and lipid to peptide ratios for the partitioning of model peptides to POPC SUV, 25°C

Peptide	$K_p \times 10^{-5}$	Number of Peptides/SUV[b]	Number of Outer Leaflet POPC/Peptide[c]
18A	4 ± 1	4	300
Ac-18A-NH_2	14 ± 4	12	110
Ac-18R-NH_2	2 ± 1	3	370
37pA	7 ± 1	7	180
37aA	5 ± 1	6	200

[a]Results given ± SD; number of experiments ≥ 3.

[b]This ratio, obtained under saturating conditions, is numerically equal to $[P_L](POPC/SUV)/[POPC]$, where $[P_L]$ is the difference between the total and free peptide concentrations, $[P] - [P_A]$ (see Appendix for calculation of $[P_A]$).

[c]The numerator is taken to be 60% of the total [POPC], (60% is the ratio of the area of the outer leaflet of a sphere of 20 nm diameter to the total area of the outer and inner leaflets). The denominator is $[P_L]$ (see footnote *b*).

TABLE 2. Thermodynamic parameters for the partitioning of model peptides to POPC SUV, 25°C

Peptide	ΔG^0	ΔH	ΔS^0
	kcal/mol		*cal/(mol K)*
18A	−7.6 ± 0.2	−11.3 ± 0.4	−12 ± 2
Ac-18A-NH_2	−8.4 ± 0.2	−15.8 ± 0.3	−25 ± 1
Ac-18R-NH_2	−7.3 ± 0.3	−17.1 ± 0.6	−33 ± 2
37pA	−7.9 ± 0.1	−25 ± 2	−56 ± 8
37aA	−7.7 ± 0.1	−21 ± 3	−45 ± 10
36A	ND	−12.6 ± 0.8	ND

Results given as means ± SD; ND, not determined.

blocked peptides (Ac-18A-NH_2 and Ac-18R-NH_2) at saturation ($F_L/F_B = F_{max}$). These differences in F_{max} values indicate that the Trp residues of the various peptides are exposed to environments of differing polarity, although it should not be inferred that these differences are directly related to differences in depth of penetration of peptides into the bilayer. Somewhat qualitative measures of partitioning/penetration are the corresponding blue shifts in the emission maxima. These shifts, together with the absolute λ_{max} in the absence and presence of lipid, are shown in **Table 3.** Also shown are data for a control, N-acetyltryptophanamide (NATA).

In order to obtain a more reliable measure of relative extents of bilayer penetration for each peptide, fluorescence quenching experiments were performed. Similar experiments have been performed by Mishra et al. (29) for Ac-18A-NH_2 and Ac-18R-NH_2 with 1,2-dimyristoyl-*sn*-glycero-3-phosphocholine (DMPC) MLV. The water-soluble quenchers iodide (I^-) and acrylamide were used for these experiments (20). Susceptibility to quenching by both should be inversely related to depth of penetration. Quenching by either I^-, with a formal negative charge, or acrylamide, which is relatively large and polar, is known to be limited to surface Trp (30); neither is capable of quenching fluorescence from buried Trp residues in globular proteins The quenching data are expressed as Stern-Volmer plots, which present fluorescence intensities as a function of quencher concentration. The experimental parameter derived from a typical Stern-Volmer plot is K_{SV} the Stern-Volmer constant (see Materials and Methods). For dynamic quenching the parameter of interest is k_q, the bimolecular rate constant for quenching, which is related to K_{SV} by $K_{SV} = k_q T_o$, where T_o is the fluorescence lifetime in the absence of quencher. Assuming T_o to be constant for the various peptides, K_{SV} is thus a convenient measure for determining relative differences in quencher accessibility to Trp when the peptides are partitioned into the bilayer. As K_{SV} is directly proportional to k_q, smaller values of K_{SV} indicate greater penetration into the bilayer. Typically, when static quenching is observed in addition to dynamic quenching, the contribution of each can be determined with the modified Stern-Volmer equation (Eq. 4, Materials and Methods). The Stern-Volmer plots for the five peptides are shown in **Fig. 3** and **Fig. 4,** along with those for indole. It has been observed that only 10–40% of the nonpolar surface of indole is buried in the bilayer, suggesting its location at the hydrocarbon-water interface (31). The indole experiments then constitute a control which should be useful in gauging relative depths of penetration.

TABLE 3. Tryptophan emission maxima of the model peptides and the model peptide-POPC complexes

Peptide[a]	Emission λ_{max}[b]			
	Buffer	POPC Complex	Blue Shift	POPC/Peptide[c]
	nm		*nm*	*mol/mol*
18A	348	334	14	550
Ac-18A-NH_2	360	336	24	190
Ac-18R-NH_2	348	334	14	550
37pA	335	332	3	340
37aA	335	332	3	340
NATA[d]	350	346	4	550

[a]Peptide concentration was 6 μM.
[b]Emission maxima were measured using an excitation wavelength of 295 nm.
[c]Ratios determined from total [POPC] and [P_L] at saturation (see footnote *c*, Table 1).
[d]N-acetyltryptophanamide.

The most straightforward interpretation of a linear Stern-Volmer plot for an efficient quencher is in terms of a collisional-quenching mechanism, in which case the slope, K_{SV}, is a measure of the collisional-quenching constant (see Eq. 3) (20). However, most of the curves in Figs. 3 and 4 exhibit at least some degree of either upward or downward curvature. Stern-Volmer plots for I^- quenching, with few exceptions, exhibit downward curvature (Fig. 3), which is typical for this quencher (23). The deviation from linearity is not great, however, and approximate K_{SV} values were determined from initial slopes. The quenching of NATA fluorescence by acrylamide has been studied by others (32). Upward curvature in this case has been interpreted as the presence of a static-quenching component, in addition to a collisional component, which at higher concentrations is due to acrylamide molecules being adjacent to the fluorophore at the moment of excitation, but which does not involve formal complexation. If this interpretation is correct, then analysis of the upward curvature in the plots of Fig. 4A according to the modified Stern-Volmer equation is appropriate (20, 23). The Stern-Volmer plots for quenching by acrylamide in the presence of vesicles (Fig. 4B) exhibit less curvature than

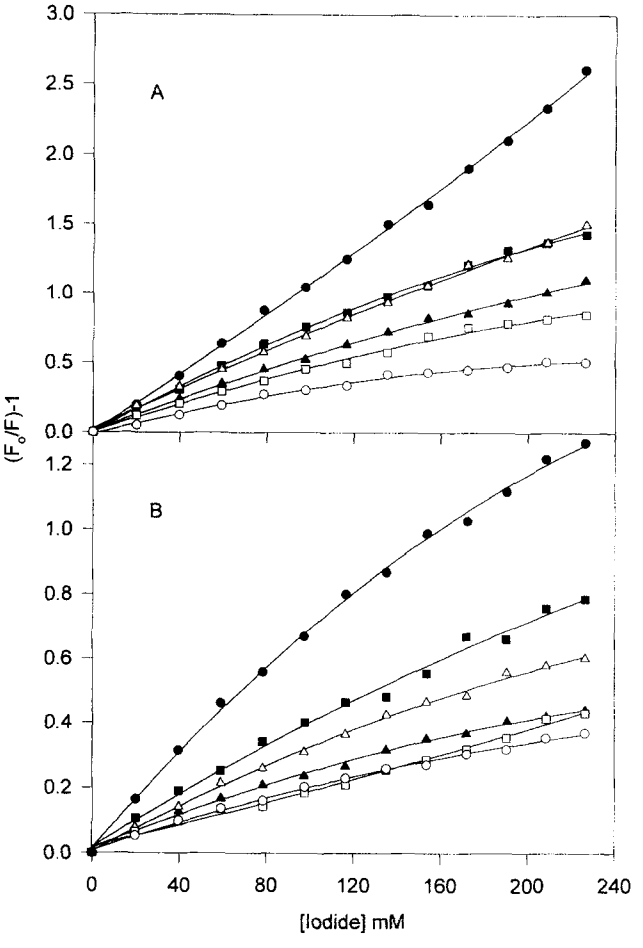

Fig. 3. Stern-Volmer plots of fluorescence quenching of the model peptides by iodide at 25°C in (A) buffer and (B) complexed with POPC. Peptide concentration was 6 μM. The excitation wavelength was 295 nm and fluorescence intensities were measured at the emission maxima (332 nm ≤ λ_{max} ≤ 360 nm). POPC/peptide molar ratios and λ_{max} values are given in Table 3. 18A (■), Ac-18A-NH_2 (▲), Ac-18R-NH_2 (△), 37pA (□), 37aA (○), NATA (●) and Indole (◆).

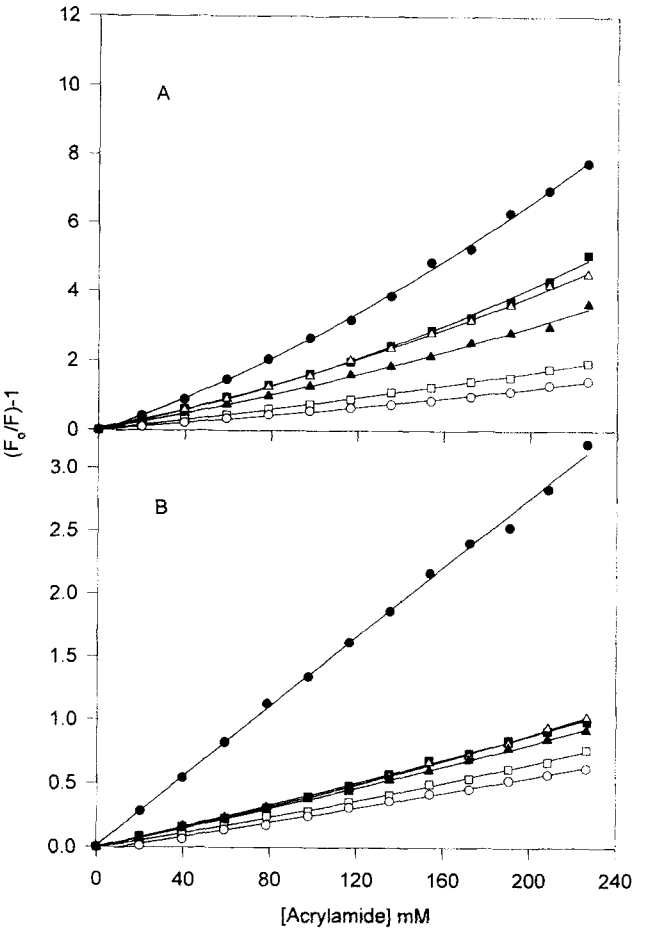

Fig. 4. Stern-Volmer plots of fluorescence quenching of the model peptides by acrylamide at 25°C in (A) buffer and (B) complexed with POPC. See legend of Fig. 3 for details.

those in buffer alone. These plots suggest that the bilayer prevents the occurrence of a static-quenching component, and also that the bilayer is unable to completely prevent collisional quenching. This is supported by the K_{SVC}/K_{SVP} ratios in **Table 4,** which may be taken as measures of $k_{q,C}/k_{q,P}$, the ratios of collisional-quenching constants in the presence and absence of vesicles. As no K_{SVC}/K_{SVP} ratio is lower that about 0.3, the presence of vesicles results in a decrease in the collisional-quenching constant by no more than about 70%. This is to be compared to quenching of fluorescence by acrylamide in proteins containing a single Trp residue, where complete burial of Trp has been shown to reduce k_q by 2 orders of magnitude. The K_{SV} values for Ac-18A-NH_2 and Ac-18R-NH_2 in buffer (**Table 5**) are similar to those obtained by Mishra et al. (29) in buffer. For peptides complexed with lipid, the two sets of data both exhibit a decrease in K_{SV} values although they differ because the lipid systems differ (highly curved SUV vs. MLV with low curvature). It is also of interest to note that K_{SV} for indole in the presence of vesicles is only slightly larger than values for lipid-associated peptides.

K_{SV} ratios obtained as described above are not statistically different for the various peptides, with the exception of that for 37aA, which exhibits a larger ratio than the other peptides (Table 4). The data suggest that the membrane gives approximately equal, but somewhat limited, protection against quenching for 18A, Ac-18A-NH_2, Ac-18R-NH_2, and 37pA, and somewhat less for 37aA. The K_{SV} values given in Table 5 indicate, however, that all the peptides appear to possess an intrinsic, intramolecular protection against quenching when

TABLE 4. Stern-Volmer quenching constants of peptide-POPC complexes relative to Stern-Volmer quenching constants of peptides in buffer

Peptide	K_{SVC}[a]/K_{SVP}[b] Iodide[c]	Acrylamide[c]
18A	0.52 ± 0.06	0.35 ± 0.07
Ac-18A-NH_2	0.46 ± 0.09	0.29 ± 0.01
Ac-18R-NH_2	0.47 ± 0.07	0.31 ± 0.02
37pA	0.39 ± 0.14	0.39 ± 0.04
37aA	0.60 ± 0.12	0.56 ± 0.02
NATA	0.64 ± 0.08	0.68 ± 0.10

[a] K_{SVC} is the Stern-Volmer quenching constant of peptide-POPC complex.
[b] K_{SVP} is the Stern-Volmer quenching constant of peptide in buffer.
[c] Values calculated from data in Table 4, ± SD.

compared to the control, NATA (Figs. 3A, 4A). This self-protection effect is greatest for the 37-residue peptides and least for 18A. A useful parameter for learning about protection conferred by the bilayer, hence about depth-of-penetration, should be a ratio of K_{SV} obtained in the presence of vesicles (K_{SVC}) to that obtained in buffer alone (K_{SVP}), which effectively normalizes information about bilayer protection to the self-protection effect. These ratios are given in Table 4.

Calorimetric studies were conducted in order to complete the thermodynamic analysis. For these experiments peptides at initial concentrations between 350 and 400μM were injected from a syringe in 10-μl aliquots into a 1.365-ml cell containing an excess of lipid to ensure essentially complete binding of peptide. In the syringe, prior to injection, peptides (P) are self-associated (P_n). It is assumed that peptide aggregates must dissociate before partitioning into the membrane occurs, or

$$P_{n(aq)} \rightleftarrows nP_{(aq)} \rightleftarrows nP_{lipid} \qquad Eq.\ 7)$$

TABLE 5. Stern-Volmer quenching constants of the model peptides in buffer and the model peptide-POPC complexes

Peptide[a]	K_{SV} (M^{-1})[b] Iodide Buffer	Iodide POPC Complex[c]	Acrylamide Buffer	Acrylamide POPC Complex[c]
18A	8.0 ± 0.4	4.2 ± 0.4	11 ± 2	3.9 ± 0.2
Ac-18A-NH_2	5.7 ± 0.3	2.6 ± 0.5	12.6 ± 0.3	3.7 ± 0.1
Ac-18R-NH_2	7.2 ± 0.9	3.4 ± 0.3	13 ± 1	4.0 ± 0.1
37pA	4.6 ± 0.5	1.8 ± 0.6	7.9 ± 0.3	3.1 ± 0.3
37aA	3.5 ± 0.3	2.1 ± 0.4	5.9 ± 0.2	3.3 ± 0.1
NATA	11.2 ± 0.7	7.2 ± 0.8	21 ± 3	14.3 ± 0.5
Indole	ND[d]	2.5 ± 1	ND	5.2 ± 0.6

[a] Peptide concentration was 6 μM.
[b] ± SD, number of experiments = 3.
[c] POPC/peptide molar ratios are given in Table 3.
[d] Not determined.

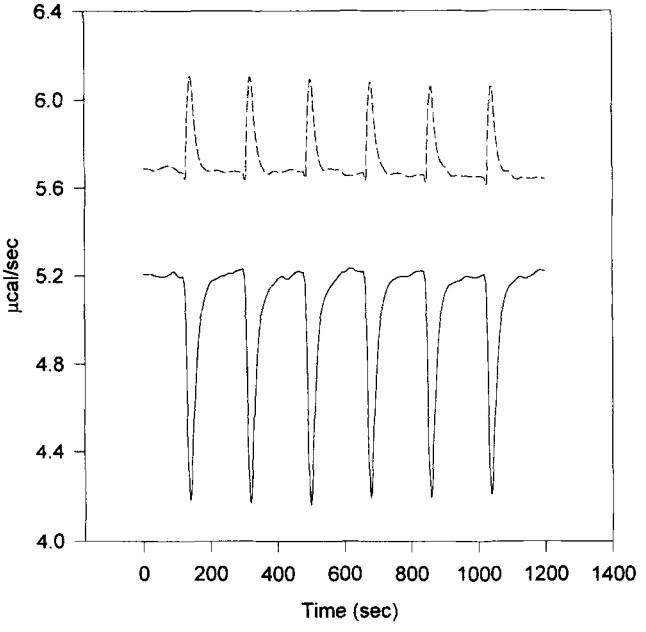

Fig. 5. Thermograms for the dissociation of 18A and binding of 18A to SUV at 5°C. The endotherms (---) for the dissociation were obtained by injecting 10 μL aliquots of a 360 μM solution of 18A into PBS. The exotherms (—) for the binding to SUV were obtained by injecting 10 μL aliquots of a 360 μM solution of 18A into an excess of lipid (>16mM, see Materials and Methods).

Figure 5 shows a typical thermogram for the partitioning of 18A into POPC SUV, together with a control in which peptide was titrated into buffer only. As peptide concentrations in the calorimeter cell were similar to those in the fluorescence experiments, at which peptides are monomeric, as mentioned previously, controls yield the heat of dissociation of peptide aggregates to monomers. Dissociation is seen to be an endothermic process, whereas the enthalpy for the entire process depicted by Eq. 7 is exothermic. The enthalpy of partitioning, ΔH, can be calculated from $\Delta H = \Delta H_{obs} - \Delta H_{diss}$ where ΔH_{obs} is the observed enthalpy of partitioning and ΔH_{diss} the enthalpy of dissociation of self-associated peptides. The standard entropy, ΔS^o, of partitioning was obtained by using $\Delta S^o = -(\Delta G^o - \Delta H^o)/T$. It is assumed that ΔH^o is approximately equal to ΔH. These thermodynamic parameters are summarized in Table 2.

In order to determine the secondary structure of the peptides their far-UV CD spectra were recorded in

TABLE 6. α-Helix content of model peptides in buffer and complexed with POPC, 25°C

Peptide	% Helicity		Δ in % Helicity	Increase in Number of Helical Residues	$\Delta S°_{\Delta Helix}$[a]	$\Delta H_{\Delta Helix}$[b]	% of Total ΔH Due to Δhelix
	Buffer	POPC Complex					
					cal/mol K	*kcal/mol*	
18A	13	49	36	6.5	−26.6	−8.4	75
Ac-18A-NH_2	38	56	18	3.2	−13.1	−4.2	26
Ac-18R-NH_2	14	62	48	8.6	−35.3	−11.2	65
37pA	26	42	16	5.9	−24.2	−7.7	31
37aA	28	49	21	7.8	−32.0	−10.1	48

[a] $\Delta S°_{\Delta Helix}$ = −4.1 e.u./residue (increase in number of helical residues), see Discussion.
[b] $\Delta H_{\Delta Helix}$ = −1.3 kcal/(mol of residue) (increase in number of helical residues), see Discussion.

buffer and when complexed with POPC SUV. These results are summarized in **Table 6.**

DISCUSSION

The amphipathic helices formed by the 18-residue peptides, Ac-18A-NH_2 and Ac-18R-NH can form helices of length sufficient to cover the fatty acyl chains at the edge of a bilayer disc comprised of DMPC. As discoidal particles have been suggested to be the nascent form of HDL, and the preferred substrate for LCAT, studies of the interaction of the 18-residue peptides with phospholipids are of particular interest. The 37-residue peptides, 37pA and 37aA, which are dimers of 18A linked by either a Pro (37pA) or Ala (37aA), are of added interest because tandem duplication of amphipathic helices exists in the exchangeable apolipoproteins, as do twists between polar and nonpolar faces and turns from one helical segment to another (4). Previous studies have shown that 18A and 18R (unblocked version of Ac-18R-NH_2) both interact superficially with the bilayer surface of POPC MLV (33). Also, both 37pA and 37aA are capable of partially penetrating a lecithin monolayer, both to a significantly greater extent than 36A (13). 37pA interacts optimally with large, DMPC MLV relative to both 36A and 37aA (13).

In the present study, a combination of isothermal titration calorimetry and fluorescence spectroscopy has enabled us to obtain a comprehensive set of thermodynamic parameters that characterize the interaction of the 18- and 37-residue peptides with POPC SUV. These parameters, together with results from circular dichroism and fluorescence quenching studies, provide considerable insight regarding the molecular nature of the interaction.

Fluorescence studies show that lipid affinities are high, with partition coefficients on the order of 10^5 (Table 1). A comparison of these values indicates that affinities, for SUV, increase in the order Ac-18R-NH_2 < 18A < 37aA < 37pA < Ac-18A-NH_2. The K_p value for Ac-18A-NH_2, with the greatest lipid affinity, is 7 times larger than that for Ac-18R-NH_2, with the least. It is of interest to note that the K_p value for the interaction of 18A with POPC SUV is almost 50 times greater than the value obtained previously for binding of 18A to large, MLV, also comprised of POPC (33), thereby indicating the importance of vesicle size in determining lipid affinity. The circular dichroism studies indicate that an increase in α-helical content occurs for all peptides upon interaction with the bilayer, with the increase being greatest for Ac-18A-NH_2 (48%) and least for 37pA (16%, Table 6). Massey, Gotto, and Pownall (34) have shown that the interaction of apoA-II and apoC-III with a variety of phospholipids occurs with a release of −1.3 kcal per mole of residue converted from a random coil to α-helix. This is comparable to values determined by Chou and Scheraga (35) and Scholtz et al. (36) for similar conversions. This indicates that approximately −11.2 kcal/mol (65% of the total ΔH of partitioning) and −7.7 kcal/mol (31% of the total ΔH of partitioning) can be attributed to an increase in helicity of Ac-18R-NH_2 and 37pA, respectively, upon interaction with vesicles.

The thermodynamic data indicate that peptide-vesicle interactions are exothermic in all cases and accompanied by relatively small, negative entropy changes (Table 2). As the calorimetric data were corrected for self-association, the enthalpies in Table 2 correspond to monomeric peptides interacting with vesicles. It might appear that peptide-vesicle interaction is driven by the removal of the hydrophobic residues of monomeric peptides from exposure to water. However, such a classic hydrophobic event would be entropically driven with very little enthalpy change (37). In contrast, interactions between these peptides and highly curved bilayer surfaces are enthalpically driven, a phenomenon that

has been observed elsewhere for interaction of other amphipathic molecules with highly curved membranes (38, 39). The negative entropy changes indicate the absence of a large net release of water from hydration shells that would occur in a classic hydrophobic event, but rather are likely due to a combination of other factors, such as the statistical effect of decreasing the number of independent particles in the system, thereby decreasing the entropy; an increase in peptide helicity likewise decreases entropy. This contribution to the decrease in entropy has been estimated (40), as −4.1 entropy units (e.u., cal/(mol K)) per residue. Using this number, together with the circular dichroism results, the change in entropy due to increase in helicity varies from about −13 e.u./peptide for Ac-18A-NH_2 to about −35 e.u./peptide for Ac-18R-NH_2.

As was mentioned previously, a number of small amphiphiles, in addition to the peptides in this study, have been observed to interact with bilayer surfaces in enthalpically driven processes. A general model of interaction has been published by Pownall et al. (41). Features unique to the systems studied here are similar for all the peptides. Amounts of α-helical content vary for free peptides in the aqueous phase. The partitioning process consists of an increase in helical content, accompanied by partial penetration of the amphipathic helices beyond the polar head groups into the hydrophobic interior of the bilayer. That there is some interaction with the hydrophobic interior of the membrane is supported by the observation that the affinity of 18A for large, POPC MLV is 1–2 orders of magnitude smaller (33) than it is for smaller, more highly curved POPC SUV in which the isothermal lateral compressibility is greater and the accessibility to the fatty acyl chains correspondingly greater. However, the existence of only partial protection by the bilayer against quenching by the water-soluble quenchers I^- and acrylamide to all the peptides and to indole is consistent with the idea that peptide-membrane interaction is largely confined to the surface, with only partial penetration of the peptides beyond the polar head groups into the hydrophobic region of the bilayers. The extent of penetration is about the same for the 18-residue peptides and 37pA, but somewhat less for 37aA. The relative lack of protection for all the peptides may be due partly to the accessibility of water to the interior of the bilayer (42). This may explain, in part, why partitioning of the peptides is not an entropically driven, classic hydrophobic event. The interaction is enthalpically driven, with a significant portion of the driving force due to increased peptide helicity that occurs upon partitioning. The increase in peptide helicity is likely due to the replacement of water-peptide backbone hydrogen bonds with intrapeptide hydrogen bonds as the nonpolar side chains encounter the hydrophobic interior of the bilayer. The majority of the remainder of the enthalpy is probably due to van der Waals interactions between the phospholipid acyl chains and the nonpolar faces of the peptides (38).

The lipid affinities are high for all the model peptides. It appears that the arrangement of charge in a class A amphipathic helix (Ac-18A-NH_2) leads to greater lipid affinity than the arrangement in which charges are reversed (Ac-18R-NH_2). However, there is little difference between Ac-18A-NH_2 and Ac-18R-NH_2 with respect to bilayer penetration. The structural basis for the difference in lipid affinity is not clear. Table 2 indicates that the enthalpies of interaction for both Ac-18R-NH_2 and Ac-18A-NH_2 are similar, while the magnitude of entropy decrease is about 30% greater for Ac-18R-NH_2. The CD results indicate a much larger increase in helicity upon interaction with vesicles for Ac-18R-NH_2 (65%) than for Ac-18A-NH_2 (26%) (Table 6). According to estimates given above, enthalpic and entropic contributions to free energies due to changes in helical content essentially cancel each other. When enthalpies and entropies in Table 2 are corrected for estimated contributions due to increases in helicity, bilayer partitioning is seen to be enthalpically driven for Ac-18A-NH_2 but is favored both enthalpically and entropically for Ac-18R-NH_2, with entropy making the larger contribution.

The 37-residue peptides, 37pA and 37aA, individual segments of which form class A amphipathic helices, have K_P values comparable to each other, but less than that for Ac-18A-NH_2 and greater than that for Ac-18R-NH_2. The presence of either a Pro (37pA) or Ala (37aA) link between helical segments would impart about a 100° twist between the interfacial planes if each segment were fully helical, as mentioned above. Several residues at the center of these peptides, therefore, are probably non-helical in the presence of lipid, allowing the interfaces of the remaining helices to align tangentially to the bilayer surface, thereby minimizing contacts between the hydrophobic faces and the aqueous medium. This idea is supported by the CD results, which indicate a lower helical content for 37-residue peptide-vesicle complexes (less than 50%) than for 18-residue peptide-vesicle complexes. Although there is very little difference in lipid affinity between 37pA and 37aA for the highly curved surface of SUV, it is interesting to note that results of a previous study indicated that 37pA has a greater affinity for large, DMPC MLV than 37aA does (13). The importance of vesicle curvature in determining lipid affinity has already been mentioned above and will be emphasized in the accompanying paper.

APPENDIX

The binding of model peptides (P) to lipid has been treated as an equilibrium partitioning between the aqueous and lipid phases

$$P_{Aqueous} \rightleftarrows P_{Lipid} \qquad Eq.\ 8)$$

The partition coefficient, K_P, is defined as

$$K_P = \frac{X_P^L}{X_P^A} \qquad Eq.\ 9)$$

where X_P^L is the mole fraction of P in the lipid phase and X_P^A is the mole fraction of P in the aqueous phase.

Conservation requires that

$$[P] = [P_A] + [P_L] \qquad Eq.\ 10)$$

where [P] is the total P concentration and $[P_A]$ and $[P_L]$ are the concentrations of P in the aqueous and lipid phases respectively. The fraction of P in the aqueous phase, is

$$\varphi = \frac{[P_A]}{[P]} \qquad Eq.\ 11)$$

It has been shown that the intrinsic fluorescence intensity of model peptides in buffer, F_B, increases when partitioned into lipid (Fig. 1). The increased fluorescence intensity, F_L, is directly proportional to X_P^L. The total intensity is the sum of F_B and the fluorescence intensity of P partitioned into lipid. When the fluorescence data are plotted as F_L/F_B lipid concentration, [L], a hyperbolic curve is obtained (Fig. 2). This binding isotherm can be expressed as

$$\frac{F_L}{F_B} = C_A\varphi + C_L(1 - \varphi) \qquad Eq.\ 12)$$

where C_A and C_L are proportionality constants corresponding to P in the aqueous and lipid phases, respectively. For reasons discussed above, when [L] = 0 C_A must equal 1. At saturation $\varphi = 0$ and C_L is equal to F_{max}, where F_{max} is the value of F_L/F_B under saturating conditions. Substitution of these values for C_A and C_L into Eq. 12 gives the following equation for F_L/F_B

$$\frac{F_L}{F_B} = \varphi(1 - F_{max}) \qquad Eq.\ 13)$$

Experimentally, F_B is determined initially for a volume, V_o, of P solution in the absence of lipid. Lipid at a concentration $[L_a]$ is then added, typically in aliquots of 50–200 μL, to give a total volume of added lipid, V_a, which is used to calculate the total volume of solution, $V_t = V_o + V_a$, and the number of moles of lipid, $n_L = [L_a]V_a$. Assuming that the number of moles of P in the aqueous phase, n_P^A, is negligible compared to the number of moles of water, n_w, X_P^A becomes

$$X_P^A = \frac{n_P^A}{n_W} \qquad Eq.\ 14)$$

Using Eqs. 9, 10, and 14, the following quadratic equation for $[P_A]$ can be obtained

$$0 = [P_A]^2 - \left(\frac{55.6}{K_P} + \frac{n_L}{V_t} + [P]\right)[P_A] + \frac{[55.6][P]}{K_P} \qquad Eq.\ 15)$$

where [55.6] is the concentration of water. Substituting [L] for n_L/V_t and using the quadratic formula to solve for $[P_A]$ gives

$$[P_A] = \frac{\frac{[55.6]}{K_P} + [L] + [P] - \sqrt{D}}{2} \qquad Eq.\ 16a)$$

where D is the discriminant, given by

$$D = \left(\frac{[55.6]}{K_P} + [L] + [P]\right)^2 - \frac{4[55.6][P]}{K_P} \qquad Eq.\ 16b)$$

The negative $\sqrt{D}$ term in Eq. 16a is used to satisfy the condition $0 \leq [P_A] \leq [P]$. Dividing Eq. 16a by [P] and substituting into Eq. 13 gives an expression for the binding isotherms in terms of K_P.

$$\frac{F_L}{F_B} = \frac{\frac{[55.6]}{K_P} + [L] + [P] - \sqrt{D}}{2[P]}(1 - F_{max}) + F_{max} \qquad Eq.\ 17)$$

The K_P value for each model peptide was obtained by curve fitting the respective binding isotherm to Eq. 17.

This research was supported in part by National Institutes of Health Program Projects HL 22633 and HL 34343.

Manuscript received 20 December 1996 and in revised form 24 June 1997.

REFERENCES

1. Brewer, H. B., Jr., T. Fairwell, A. LaRue, R. Ronan, A. Hauser, and T. J. Bronzert. 1978. The amino acid sequence of human apoA-I, an apolipoprotein isolated from high density lipoproteins. *Biochem. Biophys. Res. Commun.* **80:** 623–630.
2. Segrest, J. P., R. L. Jackson, J. D. Morrisett, and A. M. Gotto, Jr. 1974. A molecular theory of lipid-protein interactions in the plasma lipoproteins. *FEBS Lett.* **38:** 247–253.
3. Segrest, J. P., H. De Loof, J. G. Dohlman, C. G. Brouillette,

and G. M. Anantharamaiah. 1990. Amphipathic helix motif: classes and properties. *Proteins*. **8:** 103–117.
4. Segrest, J. P., M. K. Jones, H. De Loof, C. G. Brouillette, Y. V. Venkatachalapathi, and G. M. Anantharamaiah. 1992. The amphipathic helix in the exchangeable apolipoproteins: a review of secondary structure and function. *J. Lipid Res*. **33:** 141–166.
5. Anantharamaiah, G. M., M. K. Jones, and J. P. Segrest. 1993. The Amphipathic helix. R. M. Epand, editor. CRC Press, Boca Raton, FL. 109–142.
6. Venkatachalapathi, Y. V., M. C. Phillips, R. M. Epand, R. F. Epand, E. M. Tytler, J. P. Segrest, and G. M. Anantharamaiah. 1993. Effect of end-group blockage on the properties of a class A amphipathic helical peptide. *Proteins*. **15:** 349–359.
7. Chung, B. H., G. M. Anantharamaiah, C. G. Brouillette, T. Nishida, and J. P. Segrest. 1985. Studies of synthetic peptide analogs of the amphipathic helix: correlation of structure with function. *J. Biol. Chem*. **260:** 10256–10262.
8. Anantharamaiah, G. M., J. L. Jones, C. G. Brouillette, C. F. Schmidt, B. H. Chung, T. A. Hughes, A. S. Bhown, and J. P. Segrest. 1985. Studies of synthetic peptide analogs of the amphipathic helix. Correlation of structure with function. *J. Biol. Chem*. **260:** 10248–10255.
9. Lund-Katz, S. L., M. C. Philips, V. K. Mishra, J. P. Segrest, and G. M. Anantharamaiah. 1995. Microenvironments of basic amino acids in amphipathic alpha helices bound to phospholipids: ^{13}C NMR studies using selectively labeled peptides. *Biochemistry*. **92:** 9219–9226.
10. Fairman, R., K. R. Shoemaker, E. J. York, J. M. Stewart, and R. L. Baldwin. 1989. Further studies of the helix dipole model: effects of a free alpha-NH_3^+ or apha-COO^- group on helix stability. *Proteins*. **5:** 1–7.
11. Jorgenson, E. V., G. M. Anantharamaiah, J. P. Segrest, J. T. Gwynne, and S. Handwerger. 1989. Synthetic amphipathic peptides resembling apolipoproteins stimulate the release of human placental lactogen. *J. Biol. Chem*. **264:** 9215–9219.
12. Nakagawa, S. H., H. S. H. Lau, F. J. Kezdy, and E. T. Kaiser. 1985. The use of polymer-bound oximes for the synthesis of large peptides usable in segment condensation: synthesis of a 44 amino acid amphiphiic peptide model of apolipoprotein A-I. *J. Am. Chem. Soc*. **107:** 7087–7092.
13. Mishra, V. K., M. M. Palgunachari, S. Lund-Katz, M. C. Phillips, J. P. Segrest, and G. M. Anantharamaiah. 1995. Effects of the arrangement of tandem repeating units of class A amphipathic α-helices in lipid interaction. *J. Biol. Chem*. **270:** 1602–1611.
14. Roseman, M. A., B. R. Lentz, B. Sears, D. Gibbes, and T. E. Thompson. 1978. Production of large unilamellar vesicles by a rapid extrusion procedure. *Chem. Phys. Lipids*. **21:** 205–222.
15. Barenholz, Y., D. Gibbes, B. J. Litman, J. Goll, T. E. Thompson, and F. D. Carlson. 1977. A simple method for the preparation of homogeneous phospholipid vesicles. *Biochemistry*. **16:** 2806–2810.
16. McLean, L. R., and M. C. Phillips. 1982. Cholesterol desorption from clusters of phosphatidylcholine and cholesterol in unilamellar vesicle bilayers during lipid transfer or exchange. *Biochemistry*. **21:** 4053–4059.
17. Sokoloff, L., and G. H. Rothblat. 1974. Sterol to phospholipid molar ratios of L cells with qualitative and quantitative variations of cellular sterol. *Proc. Soc. Exp. Biol. Med*. **146:** 1166–1172.
18. Lehrere, S. S. 1971. Solute perturbation of protein fluorescence. The quenching of the tryptophyl fluorescence of model compounds and of lysozyme by iodide ion. *Biochemistry*. **10:** 3254–3263.
19. Calhoun, D. B., J. M. Vanderkooi, and S. W. Englander. 1983. Penetration of small molecules into proteins studied by quenching of phosphorescence and fluorescence. *Biochemistry*. **22:** 1533–1539.
20. Eftink, M. R., and C. A. Ghiron. 1981. Fluorescence quenching studies with proteins. *Anal. Biochem*. **114:** 199–227.
21. Yang, J. T., C. S. C. Wu, and H. M. Martinez. 1986. Calculation of protein conformation from circular dichroism. *Methods Enzymol*. **130:** 208–269.
22. Morrisett, J. D., J. S. K. David, H. J. Pownall, and A. M. Gotto, Jr. 1973. Interaction of an apolipoprotein (apoLP-alanine) with phosphatidylcholine. *Biochemistry*. **12:** 1290–1299.
23. Lakowicz, J. R. 1983. Principles of Fluorescence Spectroscopy. Plenum Press, New York. 187–211.
24. Trauble, H., G. Middelhoff, and V. W. Brown. 1974. Interaction of a serum apoliprotein with ordered and fluid lipid bilayers. Correlation between lipid and protein structure. *FEBS Lett*. **49:** 269–275.
25. Weinberg, R. B., and M. K. Jordan. 1990. Effects of phospholipid on the structure of human apolipoprotein A-IV. *J. Biol. Chem*. **265:** 8081–8086.
26. Weinberg, R. B., M. K. Jordan, and A. Steinmetz. 1990. Distinctive structure and function of human apolipoprotein variant apoA-IV-2. *J. Biol. Chem*. **265:** 18372–18378.
27. Seelig, J., S. Nebel, P. Ganz, and C. Bruns. 1993. Electrostatic and nonpolar peptide-membrane interactions. Lipid binding and functional properties of somatostatin in analogues of charge z = +1 to z = +3. *Biochemistry*. **32:** 9714–9721.
28. Matsuzaki, K., O. Murase, H. Tokuda, S. Funakoshi, N. Fujii, and K. Miyajir. 1994. Orientational and aggregational states of magainin 2 in phospholipid bilayers. *Biochemistry*. **33:** 3342–3349.
29. Mishra, V. K., M. M. Palgunachari, J. P. Segrest, and A. M. Anantharamaiah. 1994. Interactions of synthetic peptide analogs of the class A amphipathic helix with lipids. *J. Biol. Chem*. **269** 7185–7191.
30. Kurzban G. P., G. Gitlin, E. A. Bayer, M. Wilchek, and P. M. Horowitz. 1989. Shielding of tryptophan residues of avidin by the binding of biotin. *Biochemistry*. **28:** 8537–8542.
31. Wimley, W. C., and S. H. White. 1993. Membrane partitioning: distinguishing bilayer effects from the hydrophobic effect. *Biochemistry*. **32:** 6307–6312.
32. Eftink, M. R., and C. A. Ghiron. 1976. Fluorescence quenching of indole and model micelle systems. *J. Phys. Chem*. **80:** 486–493.
33. Spuhler, P., G. M. Anantharamaiah, J. P. Segrest, and J. Seelig. 1994. Binding of apoliprotein A-I model peptides to lipid bilayers. *J. Biol. Chem*. **269:** 23904–23910.
34. Massey, J. B., A. M. Gotto, Jr., and H. J. Pownall. 1979. Contribution of α-helix formation to their enthalpy of association with phospholipid. *J. Biol. Chem*. **254:** 9359–9361.
35. Chou, P. Y., and H. A. Scheraga. 1971. Calorimetric measurement of enthalpy change in the isothermal helix-coil transition of poly-L-lysine in aqueous solution. *Biopolymers*. **10:** 657–689.

36. Scholtz, J. M., S. Marqusee, R. Baldwin, E. J. York, J. M. Stewart, M. Santoro, and P. W. Boleri. 1991. Calorimetric determination of the enthalpy change for the α-helix to coil transition of an alanine peptide in water. *Proc. Natl. Acad. Sci. USA*. **88:** 2854–2858.
37. Tanford, C. H. 1973. The Hydrophobic Effect: Formation of Micelles and Biological Membranes. Wiley, New York. 1–3.
38. Seelig, J. P., and Ganz. 1991. Nonclassical hydrophobic effect in membrane binding equilibria. *Biochemistry*. **30:** 9354–9359.
39. Beschiaschvili, G., and J. Seelig. 1992. Peptide binding to lipid bilayers. Nonclassical hydrophobic effect and membrane-induced pK shifts. *Biochemistry*. **31:** 10044–10053.
40. Tanford, C. 1962. Contributions of hydrophobic interactions to the stability of the globular conformations of proteins. *J. Am. Chem. Soc*. **84:** 4240–4247.
41. Pownall, H. J., J. B. Massey, J. T. Sparrow, and A. M. Gotto, Jr. 1987. Plasma Lipoproteins. A.M. Gotto, Jr., editor. *Elsevier*. 95–127.
42. Jacobs, R. E., and S. H. White. 1989. The nature of hydrophobic binding of small peptides at the bilayer interface: implications for the insertion of transbilayer helices. *Biochemistry*. **28:** 3421–3437.